

An alternative comparison is of the longitudinal and transverse scans through the centres of the Bragg reflections, and these are shown in Figs. 9–11. The theoretical transverse widths are systematically smaller than the measured widths by about 20%, in reasonable agreement with the discrepancy between the Gaussian theory and the measured transverse widths shown in Fig. 2. The longitudinal widths for the 400 and 420 reflections are in good agreement with experiment but the calculation for the 440 reflection is slightly broader than expected. This may be due to a reduction in the wavelength spread caused by the positioning of the pre-monochromator slit in the experiment.

#### IV. Concluding remarks

In this paper we have presented a detailed theoretical and experimental study of the resolution function of a triple-crystal X-ray diffractometer based on a rotating-anode source. Two different theories are compared with the experimental results.

In the Gaussian approximation theory, analytic and relatively simple expressions are used to calculate the widths of the central part of the resolution function. The comparison with experiment shows that the theory predicts the widths with an accuracy of better than 25% for a variety of different diffractometer configurations. The accuracy is improved if the Darwin widths of the monochromator and analyser crystals are adjusted to fit the data at one wave-vector transfer.

A more complicated theory, involving numerical convolution of the Darwin profiles, enables the detailed form of the resolution function to be calculated in the high-resolution configuration. This theory

not only successfully describes the central part of the resolution function, but also the qualitative features of the scattered intensity away from the Bragg peak. The streaks, which appear at low intensity levels, are caused by the asymmetric form of the monochromator and analyser response functions. A simple account of the origin and direction of the streaks is given in § II.2. Unfortunately a detailed description requires a full knowledge of the monochromator and analyser response functions. These depend critically on the surface roughness of the crystals which is not usually controlled in an experiment.

We are grateful for the technical support of H. Vass, and for the financial support of the Science and Engineering Research Council.

#### References

- ANDREWS, S. R. & COWLEY, R. A. (1985). *J. Phys. C*, **18**, 6427–6439.  
 ANDREWS, S. R. & COWLEY, R. A. (1986). *J. Phys. C*, **19**, 615–635.  
 BATTERMAN, B. & COLE, H. (1964). *Rev. Mod. Phys.* **36**, 681–717.  
 BJERRUM-MØLLER, H. & NIELSEN, M. (1970). *Instrumentation for Neutron Inelastic Scattering Research*, pp. 49–76. Vienna: International Atomic Energy Agency.  
 CHESSER, N. J. & AXE, J. D. (1973). *Acta Cryst.* **A29**, 160–169.  
 COOPER, M. J. & NATHANS, R. (1967). *Acta Cryst.* **23**, 357–367.  
 COWLEY, R. A. (1987). *Acta Cryst.* **A43**, 825–836.  
 COWLEY, R. A. & RYAN, T. W. (1987). *J. Phys. D*, **20**, 61–68.  
 GARTSTEIN, E. (1989). In preparation.  
 PYNN, R., FUJII, Y. & SHIRANE, G. (1983). *Acta Cryst.* **A39**, 38–46.  
 ROBINSON, I. K. (1986). *Phys. Rev. B*, **33**, 3830–3836.  
 RYAN, T. W. (1986). PhD thesis. Univ. of Edinburgh, Scotland.  
 RYAN, T. W., NELMES, R. J., COWLEY, R. A. & GIBAUD, A. (1986). *Phys. Rev. Lett.* **56**, 2704–2707.  
 STEDMAN, R. (1968). *Rev. Sci. Instrum.* **39**, 878–883.  
 ZACHARIASEN, W. H. (1945). *Theory of X-ray Diffraction in Crystals*. New York: Wiley.

*Acta Cryst.* (1989). **A45**, 422–427

### Distortion of the Zeroth-Order Laue-Zone Pattern Caused by Dislocations in a Silicon Crystal\*

BY JIANGUO WEN, RENHUI WANG AND GANGHUA LU†

*Department of Physics, Wuhan University, 430072 Wuhan, People's Republic of China*

(Received 7 November 1988; accepted 18 January 1989)

#### Abstract

The effect of dislocations in a silicon single crystal on the zeroth-order Laue-zone (ZOLZ) pattern

in large-angle convergent-beam electron diffraction (LACBED) has been studied experimentally. It is found that edge dislocations cause the ZOLZ pattern to be compressed or elongated and screw dislocations cause it to be dislocated. This phenomenon is the consequence of opposite shifts of the two halves of the Tanaka pattern, separated by the shadow image of the dislocation line along directions  $\mathbf{b}$  and  $-\mathbf{b}$  of the Burgers vector. The shift direction of each half

\* Project supported by the National Natural Science Foundation of China.

† Also with Laboratory of Atomic Image of Solids, Institute of Metal Research, Academia Sinica, 110015 Shenyang, People's Republic of China.

of the pattern depends on the dislocation characteristics and the position of the incident-beam crossover. The pattern on the side, pointed to by the vector  $\mathbf{u} \times \mathbf{c}$  (or  $-\mathbf{u} \times \mathbf{c}$ ) from the shadow image of the dislocation line is shifted along  $\mathbf{b}$  (or  $-\mathbf{b}$ ), where  $\mathbf{u}$  is the direction of the dislocation-line vector and  $\mathbf{c}$  is a vector pointing to the beam crossover from the dislocation line. This phenomenon can be used to determine the Burgers vector (both its direction and sense) of a dislocation.

### 1. Introduction

Carpenter & Spence (1982) and Fung (1985) studied the splitting of some higher-order Laue-zone (HOLZ) lines induced by dislocations in silicon by means of convergent-beam electron diffraction (CBED) and pointed out that this phenomenon can be interpreted by the diffraction-contrast theory and can be used to determine the direction of the Burgers vector of the dislocation. Cherns & Preston (1986), Tanaka (1986) and Tanaka, Terauchi & Kaneyama (1988) discussed an excellent method to determine the Burgers vector of a dislocation by using the splitting of HOLZ lines in the hole strain field of the dislocation. Carpenter & Spence (1982) also showed that the symmetry of the zeroth-order Laue-zone (ZOLZ) pattern in the central disc is severely perturbed when the incident probe is positioned over a dislocation, whereas Bian (1986) reported a phenomenon that dislocations in a subgrain boundary of pure aluminium cause the ZOLZ pattern to be regularly dislocated. A similar phenomenon was discussed by Cherns, Kiely & Preston (1988) who observed that some diffraction fringes in the Tanaka pattern are displaced in opposite directions on opposite sides of the shadow image of misfit dislocations in  $\text{NiSi}_2/(111)\text{Si}$  foils. The purpose of this work is to explore the factors controlling the distortion of the ZOLZ pattern caused by dislocations, including the character of the given dislocation, the sense of its Burgers vector and the position of the incident-beam crossover.

### 2. Experimental method

Two methods were used to introduce dislocations into perfect silicon single crystals. In the first method a silicon plate was bent under three-point loading at 1170 K; in the second method a series of microhardness indentations were made at separations of twenty times the indentation diameter. Transmission electron microscopy (TEM) specimens were prepared from the deformed silicon by means of mechanical grinding and polishing, and then by ion-milling.

The irradiated diameter in the large-angle CBED (LACBED) (Tanaka, Saito, Ueno & Harada, 1980) is considerable (some micrometres) and different positions of a LACBED pattern (Tanaka pattern) reflect the structure information of different positions

of the irradiated area. In the LACBED method, one can accurately select the diffraction area by means of the shadow image of a dislocation line and study the elastic strain field on both sides of the dislocation.

The line direction  $\mathbf{u}$  and the Burgers vector  $\mathbf{b}$  of a dislocation, which are defined according to the FS/RH (perfect crystal) convention (e.g. Hirsch, Howie, Nicholson, Pashley & Whelan, 1977), were determined in this work by means of diffraction contrast and trace analysis. According to Hirsch *et al.* (1977), the diffraction-contrast image of a dislocation deviates from the real dislocation line when  $\mathbf{g} \cdot \mathbf{b} \neq 0$  and  $s_g \neq 0$  with  $\mathbf{g}$  the diffraction vector and  $s_g$  its excitation error. The image is at the side pointed to by the vector  $\mathbf{u} \times \mathbf{B}$  (or  $-\mathbf{u} \times \mathbf{B}$ ) from the dislocation line when  $(\mathbf{g} \cdot \mathbf{b})s_g > 0$  [or  $(\mathbf{g} \cdot \mathbf{b})s_g < 0$ ], where the vector  $\mathbf{B}$  is along the incident electron beam. Therefore, from two  $+\mathbf{g}$  and  $-\mathbf{g}$  diffraction-contrast images of a dislocation, marked by contamination reference spots, the direction and sense of the Burgers vector  $\mathbf{b}$  of this dislocation can be determined. According to the conventional definition (Hull & Bacon, 1984), an edge dislocation is called positive (or negative) if its extra half-plane of atoms is above (or below) the dislocation line. The sign of an edge dislocation can be deduced from its  $\mathbf{u}$  and  $\mathbf{b}$  because the vector  $\mathbf{u} \times \mathbf{b}$  points to the extra half-plane of atoms. A screw dislocation is called right handed (or left handed) if its  $\mathbf{b}$  is parallel (or anti-parallel) to  $\mathbf{u}$ . Therefore, the handedness of a screw dislocation is easily determined from its  $\mathbf{u}$  and  $\mathbf{b}$ .

### 3. Experimental results

#### 3.1. Edge dislocation

Figs. 1(a) and (b) are [001] Tanaka patterns at 80 kV, with the central incident beam placed on the core (Fig. 1a) and on the right-hand side (Fig. 1b) of a vertical edge-dislocation line marked with the vector  $\mathbf{u}$ . In both cases the beam crossover was below the TEM specimen. Diffraction-contrast analysis revealed that this is a negative edge dislocation with  $\mathbf{u} \parallel [110]$  and  $\mathbf{b} \parallel [1\bar{1}0]$ . It is discernible on comparing Figs. 1(a) and (b) that the Tanaka patterns at the right-hand and left-hand sides of the dislocation line are shifted towards each other along the direction perpendicular to the dislocation line, *i.e.* along the  $\mathbf{b}$  and  $-\mathbf{b}$  directions, respectively. This effect gives an impression that the Tanaka patterns are compressed.

#### 3.2. Screw dislocation

Fig. 2(a) shows a [001] Tanaka pattern. The right-hand and left-hand parts of the pattern are dislocated along the vertical boundary which is the shadow image of a screw dislocation. Fig. 2(b) shows another [001] Tanaka pattern. Near the centre of this pattern

is one end of a screw dislocation ( $\mathbf{u} \parallel \mathbf{b} \parallel [110]$ ) which extends into the upper part of the pattern. The lower half of this pattern is not affected by the presence of the screw dislocation but the right-hand and left-hand parts of the upper half of this pattern are dislocated along the direction of the screw dislocation line, namely along  $\mathbf{b}$  and  $-\mathbf{b}$  directions respectively. In this case the diffraction fringes in the ZOLZ pattern appear as a single screw. In some other cases the ZOLZ pattern may appear as a double screw when a screw dislocation extends across the whole pattern and the relative shift of the two parts of the pattern is approximately equal to the spacing of the fringes.

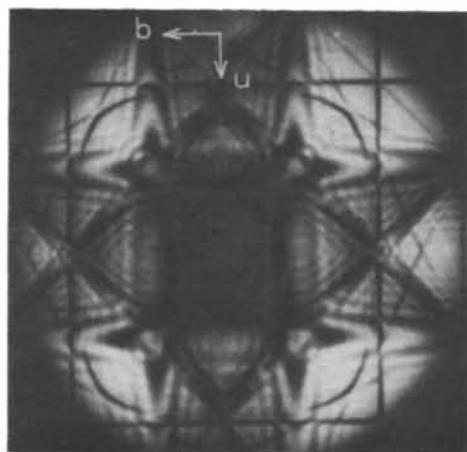
### 3.3. Mixed dislocation

Fig. 3(a) shows the diffraction-contrast image of a dislocation with the incident beam nearly parallel to the [001] direction. Diffraction-contrast analysis

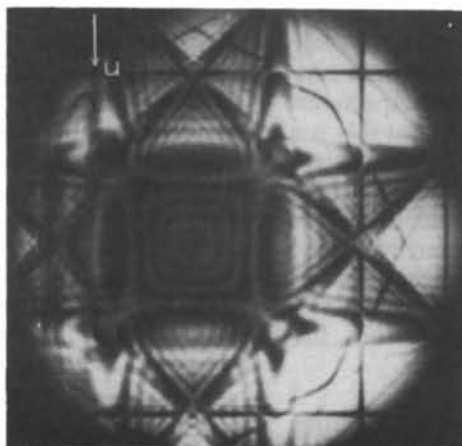
revealed that it is a  $70^\circ$  dislocation with  $\mathbf{b} \parallel [1\bar{1}0]$ . Figs. 3(b) and (c) show [001] Tanaka patterns at 80 kV, with the central incident beam placed on this dislocation line (Fig. 3(b)) and on its right-hand side (Fig. 3(c)). In both cases the beam crossover was below the TEM specimen. The contamination spots in Fig. 3 help to discern the position of the dislocation line in the Tanaka patterns. By comparing Figs. 3(b) and (c), one can see the ZOLZ patterns at the right-hand and left-hand sides of the dislocation line are shifted approaching each other along the  $\mathbf{b}$  and  $-\mathbf{b}$  directions respectively, which results in the pattern appearing to be compressed.

### 3.4. Effect of the level of beam crossover

Figs. 4(a), (b) and (c) are a series of [001] CBED patterns at the same negative edge-dislocation line with the incident-beam crossover placed well above

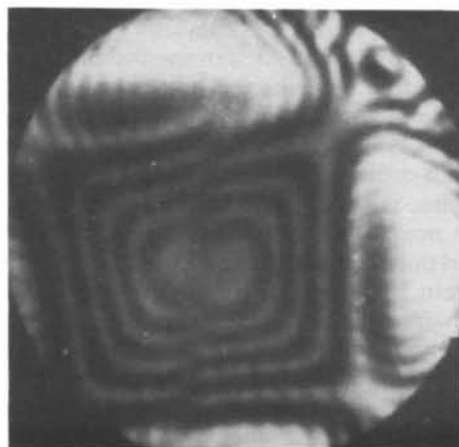


(a)

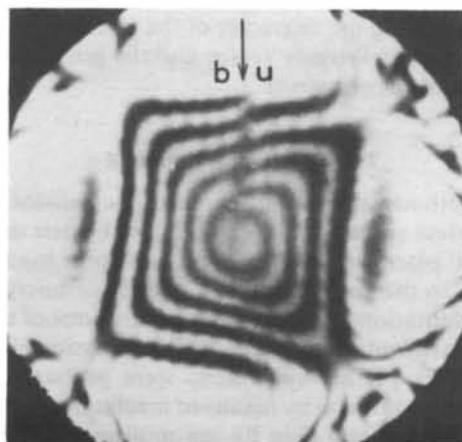


(b)

Fig. 1. Si [001] Tanaka patterns at 80 kV with a vertical edge-dislocation line (a) in the central part and (b) at the left-hand side.

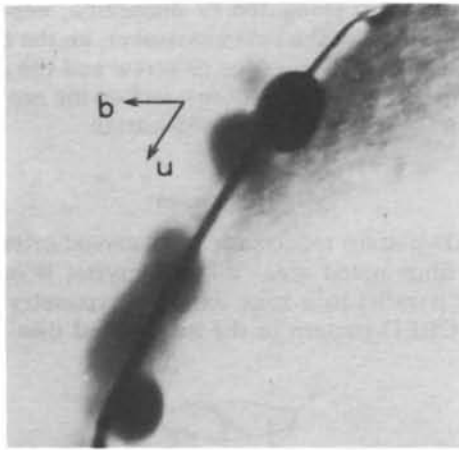


(a)

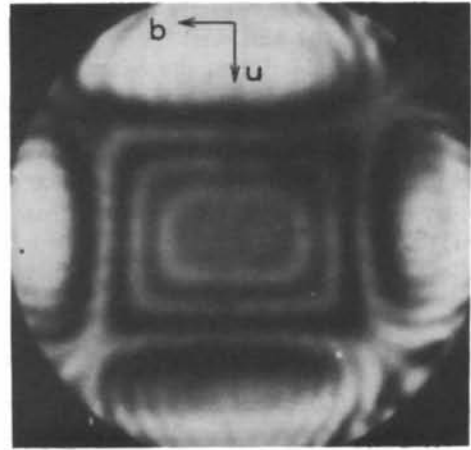


(b)

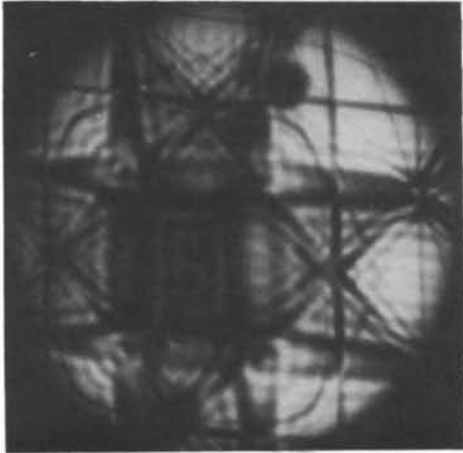
Fig. 2. Si [001] Tanaka patterns at 120 kV with a vertical screw dislocation (a) across the whole pattern and (b) extending from the centre to the upper part.



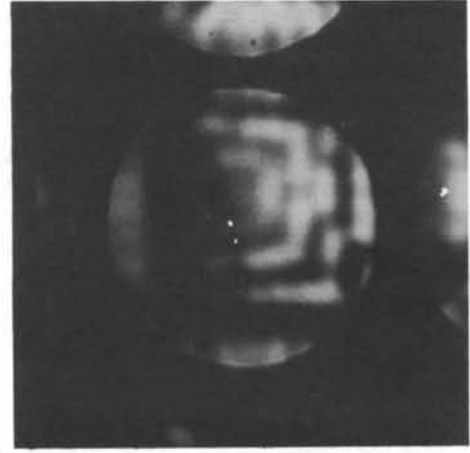
(a)



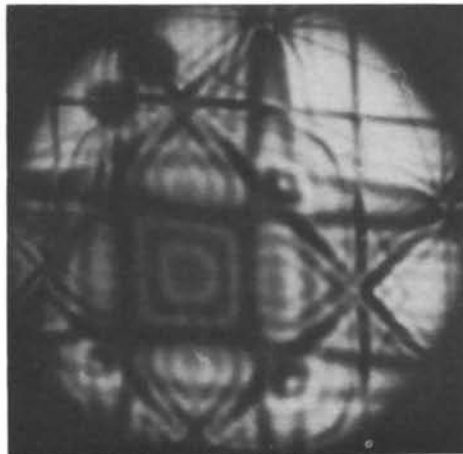
(a)



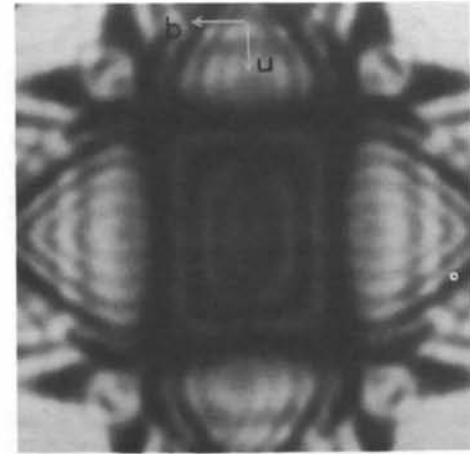
(b)



(b)



(c)



(c)

Fig. 3. Effect of a mixed dislocation on the Tanaka pattern. (a) Dislocation-contrast image of a  $70^\circ$  dislocation in silicon with contamination reference spots. (b), (c) [001] Tanaka patterns at 80 kV.

Fig. 4. [001] CBED patterns of silicon containing a vertical negative edge dislocation, with the beam crossover (a) above the specimen, (b) on the core of the dislocation and (c) below the specimen.

the specimen (Fig. 4a), exactly on the core of the dislocation (Fig. 4b) and well below the specimen (Fig. 4c) respectively. When the beam crossover is exactly on the core of the dislocation, the ZOLZ pattern in the CBED appears severely distorted without any regular compression or elongation, see Fig. 4(b), as was observed by Carpenter & Spence (1982). By changing the beam crossover from above (Fig. 4a) to below (Fig. 4c) the specimen, the character of the Tanaka pattern changes from elongation to compression.

### 3.5. Effect of turning the specimen upside down

Fig. 5 shows a [001] Tanaka pattern with the same edge-dislocation line as in Fig. 4(a) after turning the TEM specimen upside down. Thus the sign of the edge dislocation is changed from negative to positive. In both cases the beam crossover is above the specimen. The Tanaka pattern as shown in Fig. 5 appears to be compressed along the **b** direction compared with the elongated pattern shown in Fig. 4(a).

On the other hand, our experiment shows that a screw dislocation causes the Tanaka pattern to be dislocated in the same way before and after turning the TEM specimen upside down (about an arbitrary axis in the specimen plane) when other experimental conditions remain unchanged. This is because the handedness (left or right) of a screw dislocation remains unchanged by turning the TEM specimen upside down, unlike the sign (positive or negative) of an edge dislocation.

In summary, the experiments described above show that a dislocation causes the two parts of a Tanaka pattern, with the shadow image of the dislocation line as their boundary, to be shifted along **b** and  $-\mathbf{b}$  directions respectively, hence causing the pattern to

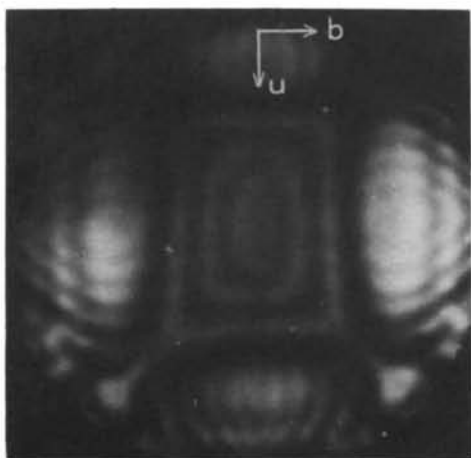


Fig. 5. [001] Tanaka pattern of silicon containing a vertical positive edge dislocation with the beam crossover above the specimen. Compare with Fig. 4(a).

be compressed, elongated or dislocated, dependent on the position of the beam crossover, on the character of the dislocation (edge or screw and the sign or handedness of the dislocation), and on the projection direction of **u** and **b** of the dislocation.

## 4. Discussion

A CBED pattern reflects the local crystal orientation of the illuminated area. When a crystal is oriented exactly parallel to a zone axis, the symmetry centre of the CBED pattern in the transmitted disc (bright

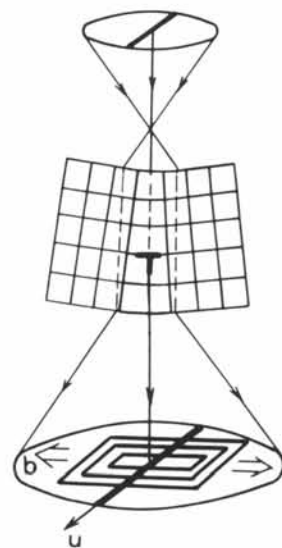


Fig. 6. Schematic diagram showing that an edge dislocation causes the Tanaka pattern to be compressed or elongated.

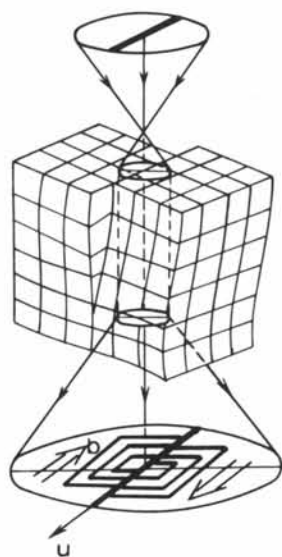
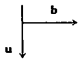
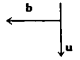
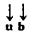
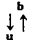
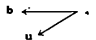


Fig. 7. Schematic diagram showing that a screw dislocation causes the Tanaka pattern to be dislocated.

Table 1. Shift direction of the Tanaka pattern caused by a dislocation

Dislocation feature	Position of the beam crossover	Shift direction of the Tanaka pattern	Examples	
Positive edge ( $\perp$ )		Above Below	$\Rightarrow \Leftarrow$ $\Leftarrow \Rightarrow$	Fig. 5 $\mathbf{u} \parallel [110], \mathbf{b} \parallel [\bar{1}10]$
Negative edge ( $\top$ )		Above Below	$\Leftarrow \Rightarrow$ $\Rightarrow \Leftarrow$	Fig. 4(a) Fig. 1(a) Fig. 4(c) $\mathbf{u} \parallel [110]$ $\mathbf{b} \parallel [1\bar{1}0]$
Right-handed screw		Above Below	$\Downarrow \Uparrow$ $\Uparrow \Downarrow$	Fig. 2(b) $\mathbf{u} \parallel \mathbf{b} \parallel [110]$
Left-handed screw		Above Below	$\Uparrow \Downarrow$ $\Downarrow \Uparrow$	
Mixed		Above Below	$\Leftarrow \Rightarrow$ $\Rightarrow \Leftarrow$	Fig. 3 $\mathbf{b} \parallel [1\bar{1}0]$

field), corresponding to the intersection of the zone axis with the photographic plate, coincides with the centre of the disc, corresponding to the intersection of the central incident beam with the photographic plate. If the crystal is tilted away, the symmetry centre of the CBED pattern shifts from the disc centre correspondingly. Different positions in a Tanaka pattern reflect the orientations of different positions of the irradiated area. When the beam crossover is above (below) the specimen, the CBED pattern on one side of the shadow image of a dislocation line reflects the orientation of the same (opposite) side of the irradiated area.

Because conventional TEM foils are not too thick, an edge dislocation which is approximately parallel to the foil surface causes the crystal on the two sides of the dislocation line to be tilted in opposite directions and hence a tilt boundary forms (see Fig. 6), as in the case of the edge-dislocation wall. This produces a shift of two parts of the CBED pattern separated by the shadow image of the edge-dislocation line along respectively  $\mathbf{b}$  and  $-\mathbf{b}$  directions normal to the dislocation line, and hence causes the pattern to be compressed or elongated. Similarly, a screw dislocation produces a rotation about an axis normal to the screw-dislocation line of one-half of the crystal with respect to the other and hence a twist boundary forms (see Fig. 7). This produces shifts of two parts of the CBED pattern along  $\mathbf{b}$  and  $-\mathbf{b}$  directions parallel to the screw-dislocation line, and hence causes the pattern to be dislocated. The shift direction of each part of a Tanaka pattern depends on the feature of the dislocation (positive or negative edge dislocation, left- or right-handed screw dislocation) and the posi-

tion of the beam crossover with respect to the TEM specimen level. All cases considered are summarized in Table 1 and compared with the experimental results described in § 3.

From Table 1 we can draw the following conclusion. Let  $\mathbf{c}$  be a vector pointing from the dislocation line to the beam crossover. The CBED pattern on the side pointed to by the vector  $\mathbf{u} \times \mathbf{c}$  ( $-\mathbf{u} \times \mathbf{c}$ ) from the shadow image of the dislocation line is shifted along the  $\mathbf{b}$  ( $-\mathbf{b}$ ) direction. This conclusion can be extended to a mixed dislocation as shown in the last two rows of Table 1, and can be used to determine easily the Burgers vector of a dislocation together with its sense during the process of a TEM observation.

#### References

- BIAN, W. M. (1986). *J. Chin. Electron Microsc. Soc.* **5**, No. 3, 46. (In Chinese.)  
 CARPENTER, R. W. & SPENCE, J. C. H. (1982). *Acta Cryst.* **A38**, 55-61.  
 CHERNS, D., KIELY, C. J. & PRESTON, A. R. (1988). *Ultramicroscopy*, **24**, 355-369.  
 CHERNS, D. & PRESTON, A. R. (1986). Proc. XIth Int. Congr. Electron Microsc. Kyoto, Japan, 1986, pp. 721-722.  
 FUNG, K. K. (1985). *Ultramicroscopy*, **17**, 81-86.  
 HIRSCH, P., HOWIE, A., NICHOLSON, R. B., PASHLEY, D. W. & WHELAN, M. J. (1977). *Electron Microscopy of Thin Crystals*, pp. 265-266. Huntington, New York: Robert E. Krieger.  
 HULL, D. & BACON, D. J. (1984). *Introduction to Dislocations*, pp. 18-19. Oxford: Pergamon.  
 TANAKA, M. (1986). *J. Electron Microsc.* **35**, 314-323.  
 TANAKA, M., SAITO, R., UENO, K. & HARADA, Y. (1980). *J. Electron Microsc.* **29**, 408-412.  
 TANAKA, M., TERAUCHI, M. & KANEYAMA, T. (1988). *Convergent-beam Electron Diffraction II*, pp. 160-185. Tokyo: JEOL-Maruzen.